

FieldSimR: An R package for simulating plot data in multi-environment field trials

Christian R. Werner^{1,2*}, Dorcus C. Gemenet^{1,2} and Daniel J. Tolhurst^{3*}

¹*Accelerated Breeding Initiative (ABI), Consultative Group of International Agricultural Research (CGIAR), Texcoco, Mexico*

²*International Maize and Wheat Improvement Center (CIMMYT), Texcoco, Mexico*

³*The Roslin Institute and Royal (Dick) School of Veterinary Studies, University of Edinburgh, Easter Bush, Midlothian, United Kingdom*

Correspondence*:

Christian R. Werner

c.werner@cgiar.org

Daniel J. Tolhurst

uow.tolhurst@gmail.com

2 **Language style note: the authors prefer the article to be formatted in British English.**

3

4 **ABSTRACT**

5 This paper presents a general framework for simulating plot data in multi-environment field trials
6 with one or more traits. The framework is embedded within the R package FieldSimR, whose core
7 function generates plot errors that capture global field trend, local plot variation, and extraneous
8 variation at a user-defined ratio. FieldSimR's capacity to simulate realistic plot data makes it a
9 flexible and powerful tool for a wide range of improvement processes in plant breeding, such as
10 the optimization of experimental designs and statistical analyses of multi-environment field trials.
11 Therefore, FieldSimR provides crucial functionality that is currently missing in other software for
12 simulating plant breeding programmes. The paper includes an example simulation of a field trial
13 to evaluate a set of 100 maize hybrids for two traits across three environments. To demonstrate
14 FieldSimR's value as an optimisation tool, the simulated data set is then used to compare eight
15 spatial models for their capacity to accurately predict the maize hybrids' genetic values and to
16 reliably estimate the variance parameters of interest.

17 **Keywords:** Simulation, Spatial variation, Plot error, Multi-environment field trials

1 **INTRODUCTION**

18 This paper presents a general framework for simulating plot data in multi-environment field trials with one
19 or more traits. The framework is embedded within the R package FieldSimR, whose core function generates
20 plot errors that capture global field trend, local plot variation, and extraneous variation. FieldSimR's capacity
21 to simulate realistic plot data makes it well-suited to a wide range of improvement processes in plant
22 breeding, such as the optimization of experimental designs and statistical analyses of multi-environment
23 field trials. It is also well-suited to a range of education purposes, such as teaching the principals of spatial
24 modelling and analysing multi-environment trial data.

25 Plant breeding programmes continuously evaluate, select and release improved genotypes in order to
26 meet the complex and dynamic requirements of different customer groups, including farmers, processors
27 and end-users (Covarrubias-Pazarán et al., 2022). The resources required to compare different improvement
28 strategies in the field, however, can quickly exceed the practical possibilities of a plant breeding programme.
29 Often, multiple factors must be evaluated simultaneously over several years or even decades to identify an
30 optimised breeding strategy. This requires a pragmatic approach to identify profitable long-term strategies
31 in plant breeding programmes.

32 Simulation is a fast and cost-efficient tool for comparing different breeding strategies over time (Gaynor
33 et al., 2021). Interestingly, this is not a new concept. Simulations have been utilised by plant and animal
34 breeders for almost a century, beginning with the application of the Breeder's equation (Lush, 1937), a form
35 of deterministic simulation to predict genetic gain based on selection intensity, selection accuracy, genetic
36 variance, and generation interval. However, only recently, with the availability of modern computers
37 and flexible software have breeders and researchers been granted access to more powerful stochastic
38 simulation for optimising entire breeding programmes across multiple generations. Currently available
39 software includes QU-GENE (Podlich and Cooper, 1998), ADAM-plant (Liu et al., 2019), and ChromaX
40 (Younis et al., 2023), as well as the R packages Selection Tools (Frisch, 2023), and AlphaSimR (Gaynor
41 et al., 2021). These software applications can be used, for example, to compare different crossing and
42 selection strategies over time. They lack, however, the functionality to simulate realistic plot data in
43 multi-environment field trials. This capacity is necessary to evaluate the impact of different experimental
44 designs, multi-environment testing strategies, and statistical analyses on the performance of a breeding
45 programme.

46 The motivation to simulate realistic plot data has stemmed from the importance of spatial variation in
47 plant breeding field trials (see, for example, Wilkinson et al., 1983; Besag and Kempton, 1986; Cullis and
48 Gleeson, 1991; Rodríguez-Álvarez et al., 2018; Piepho et al., 2022). Spatial variation occurs naturally in
49 field trials laid out as a two-dimensional lattice of plots (Gogel et al., 2023), and can account for more than
50 50% of the total phenotypic variation. Spatial variation can be broadly categorised as either global trend,
51 local variation or extraneous variation (Gilmour et al., 1997). Global trend occurs on a large scale across
52 the field, such as large scale moisture and fertility gradients (Green et al., 1985). Local variation occurs on
53 a small scale between neighbouring plots. It may reflect small scale changes in soil composition (trend) or
54 random error (noise), such as measurement error and within-plot variability (Besag, 1977). Conversely,
55 extraneous variation is predominately induced during the conduct of the trial, and as a result is often
56 aligned with the columns and rows. It may reflect management practices, such as serpentine harvesting and
57 spraying, multi-plot seeders that sow multiple plots simultaneously, or inaccurate trimming resulting in
58 unequal plot lengths (Stefanova et al., 2009). The complexity and importance of spatial variation dictate
59 the need for a framework to simulate plot errors that capture the main components of spatial variation.

60 FieldSimR is an R package for simulating plot errors in multi-environment field trials that comprise global
61 and local trend, random error, and extraneous variation. It also provides compatibility with AlphaSimR
62 to simulate plot phenotypes. This makes FieldSimR a powerful tool for a wide range of improvement
63 processes, such as:

- 64 • Comparing spatial modelling approaches, e.g., separable autoregressive processes, tensor product
65 penalised splines, and nearest neighbour adjustments.
- 66 • Comparing experimental designs for single- and multi-environment studies, e.g., fully-replicated
67 designs, p -rep designs and sparse testing designs.

68 • Comparing approaches for analysing multi-environment trial data, e.g., random regressions and factor
69 analytic models.

70 The paper is arranged as follows. The Methods section presents the theoretical framework for simulating plot
71 errors, which are constructed by combining spatial error, random error, and extraneous error components at
72 a user-defined ratio. The Results and Discussion section introduces an example simulation of a field trial to
73 evaluate a set of 100 maize hybrids for two traits across three environments. To demonstrate FieldSimR's
74 value as an optimisation tool, the simulated data set is then used to compare eight spatial models for
75 their capacity to accurately predict the maize hybrids' genetic values and reliably estimate the variance
76 parameters of interest.

2 METHODS

77 This section presents the framework in FieldSimR for simulating plot errors in multi-environment field
78 trials. FieldSimR generates plot errors by combining spatial error, random error and extraneous error
79 components at a user-defined ratio. The simulation framework is initially developed for a single trait and
80 then generalised for multiple traits.

81 2.1 Framework for simulating single-trait plot errors in multi-environment field trials

82 Assume a single-trait multi-environment trial (MET) dataset comprises p environments with n plots
83 in total, where $n = \sum_{j=1}^p n_j$ and n_j is the number of plots in environment j . Also assume that each
84 environment is laid out as a two-dimensional lattice of plots such that $n_j = c_j \times r_j$, where c_j and r_j are the
85 number of columns and rows, respectively. The n -vector of plot errors is then given by $\boldsymbol{\varepsilon} = (\boldsymbol{\varepsilon}_1^\top, \dots, \boldsymbol{\varepsilon}_p^\top)^\top$,
86 where $\boldsymbol{\varepsilon}_j$ is the n_j -vector of plot errors for environment j (ordered as rows within columns). The vector
87 $\boldsymbol{\varepsilon}_j$ comprises the main components of spatial variation, i.e. global and local trend, random error, and
88 extraneous variation.

89 FieldSimR constructs the vector of plot errors as the sum of three terms:

$$\boldsymbol{\varepsilon}_j = \mathbf{s}_j + \mathbf{r}_j + \mathbf{e}_j, \quad (1)$$

90 where \mathbf{s}_j is a vector of errors that capture spatial trend, \mathbf{r}_j is a vector of random errors, and \mathbf{e}_j is a vector
91 of errors that capture extraneous variation. The errors in \mathbf{s}_j and \mathbf{e}_j are hereafter referred to as the spatial
92 and extraneous errors, respectively. All terms are simulated as mutually independent with zero means and
93 variance components given by $\sigma_{s_j}^2$, $\sigma_{r_j}^2$, and $\sigma_{e_j}^2$, respectively. The total plot error variance is then given by
94 $\sigma_{\boldsymbol{\varepsilon}_j}^2 = \sigma_{s_j}^2 + \sigma_{r_j}^2 + \sigma_{e_j}^2$.

95 2.1.1 Spatial error

96 The errors in \mathbf{s}_j capture both global and local trend, such as large scale fertility gradients (Green et al.,
97 1985) and small scale changes in soil composition (Gilmour et al., 1997). The vector \mathbf{s}_j is generated in
98 FieldSimR using either bivariate interpolation (Akima, 1978) or a separable autoregressive process (Box
99 and Jenkins, 1970).

100 Bivariate interpolation is implemented through the `interp` function in the R package `interp` (Gebhardt
101 et al., 2023), which applies piece-wise linear interpolation across the two-dimensional lattice of plots. An
102 example field array with spatial trend generated using bivariate interpolation is presented in Figure 1. The
103 field array comprises $c_j = 10$ columns and $r_j = 20$ rows for $n_j = 200$ plots in total. The field spans

104 80 m long in the column direction and 40 m wide in the row direction, with rectangular plots 8 m long
 105 by 2 m wide (Figure 1a). There are two square blocks aligned in the column direction (“side-by-side”),
 106 with 100 plots in each block. Four interpolation (knot) points are placed outside the four corners of the
 107 field, which prevents continuity issues that occur at the interpolation boundary. The z -values at these
 108 points were sampled from a standard normal distribution, with $z = 2.56, 1.08, 0.43$, and -2.56 for this
 109 example (clockwise from top left). The continuous array between the knot points is then interpolated,
 110 which produces a smooth continuous surface across the lattice of plots (Figure 1b). A single error value
 111 is assigned to each plot by averaging over the continuous surface within each plot (Figure 1c). The error
 112 values are then scaled to the defined spatial error variance for each environment, $\sigma_{s_j}^2$. This produces the
 113 vector of spatial errors, \mathbf{s}_j .

114 The complexity of spatial trend can be controlled in FieldSimR by setting the number of additional knot
 115 points sampled inside the field array. By altering the complexity, users can explicitly change the ratio
 116 of global to local trend. The example in Figure 1 has no additional knot points besides those at the four
 117 corners, so the simulated spatial error predominately captures global trend with minimal or no local trend.
 118 Three additional examples are presented in Figure 2, which have 5, 10, and 50 knot points, respectively.
 119 The knot points are sampled from a continuous uniform distribution defined by all points in the continuous
 120 array. This means that more than one knot point can be sampled for each plot. The position of the knot
 121 points and corresponding z -values are presented in Supplementary Figure S1, which displays the smooth
 122 continuous surface for the examples in Figure 2.

123 The examples demonstrate FieldSimR’s capacity to generate global and local trend, as well as within-plot
 124 variability. Increasing the complexity will generate more local trend relative to global trend, up to a point
 125 where the errors capture minimal or no trend (i.e., only noise). At this point, numerous knot points may
 126 be sampled for each plot which may further increase the amount of within-plot variability. By default,
 127 FieldSimR sets the number of knot points to half the maximum of the number of columns and rows. For
 128 example, the default complexity for a field trial with 20 columns and 10 rows is given by $\max(20, 10) / 2$
 129 $= 10$ knot points (see, for example, Figure 2b). This generally provides a good ratio of global to local
 130 trend, but users are encouraged to alter the complexity as required.

131 Trellis plots for the three examples are presented in Supplementary Figure S2. These plots also
 132 demonstrate that various ratios of global to local trend can be generated by altering the complexity. For
 133 example, the first plot demonstrates a gradual decrease in spatial error as the row number increases, which
 134 is a classical sign of global trend in field trials. In contrast, the last plot demonstrates more small-scale
 135 fluctuations between neighbouring columns and rows, which is a sign of local trend. It is important to note
 136 that bivariate interpolation is a smoothing function, rather than a stochastic process, so the errors are not
 137 simulated as random variables.

138 The separable autoregressive process simulates spatial errors as random variables based on a stochastic
 139 variance matrix. Separable autoregressive processes explicitly model spatial dependence (correlation)
 140 between neighbouring plots, rather than a smooth continuous surface across the field. In this case,
 141 FieldSimR simulates the vector of spatial errors as:

$$\mathbf{s}_j \sim \mathbf{N}(\mathbf{0}, \sigma_{s_j}^2 \mathbf{S}_j), \quad (2)$$

142 where $\sigma_{s_j}^2$ is the spatial error variance and \mathbf{S}_j is the stochastic variance matrix, which is constructed as:

$$\mathbf{S}_j = \boldsymbol{\Sigma}_{\mathbf{c}_j}(\rho_{c_j}) \otimes \boldsymbol{\Sigma}_{\mathbf{r}_j}(\rho_{r_j}), \quad (3)$$

143 where ρ_{c_j} is the column autocorrelation parameter with $c_j \times c_j$ correlation matrix Σ_{c_j} and ρ_{r_j} is the row
 144 autocorrelation parameter with $r_j \times r_j$ correlation matrix Σ_{r_j} . FieldSimR has the capacity to generate
 145 errors based on a separable first order autoregressive process (AR1). Note that, in contrast to bivariate
 146 interpolation, the autoregressive process is not based on plot dimensions, since they are implicitly modelled
 147 through ρ_{c_j} and ρ_{r_j} (see Gilmour et al., 1997). This approach allows users to implement estimates of ρ_{c_j}
 148 and ρ_{r_j} previously obtained from empirical analyses of field trial data.

149 The ratio of global to local trend can be controlled by altering the column and row autocorrelation
 150 parameters. Decreasing the autocorrelation parameters will effectively increase the complexity of the
 151 spatial trend, in the sense that more local trend will be generated relative to global trend, up to a point
 152 where the errors capture minimal or no trend (i.e., only noise). This occurs when the autocorrelation
 153 parameters are set to zero. Three examples are presented in Supplementary Figure S3, which show spatial
 154 trend generated using a separable first order autoregressive process with (a) $\rho_c = 0.7$ and $\rho_r = 0.9$, (b)
 155 $\rho_c = 0.5$ and $\rho_r = 0.7$, and (c) $\rho_c = 0.3$ and $\rho_r = 0.5$. The theoretical and sample variograms for these
 156 examples are presented in Supplementary Figure S4. These examples demonstrate the stochastic nature of
 157 the spatial errors generated based on autoregressive processes.

158 The methods above for generating global and local trend will be well-suited to most applications.
 159 However, some users may want to explicitly set the amount of global and local trend without fine-tuning
 160 the complexity or the autocorrelation parameters. In this case, users may simulate trend as the sum of
 161 two components, i.e., global trend (with no to low complexity) and local trend (with moderate to high
 162 complexity or low to moderate autocorrelations). This is left to the discretion of the user.

163 2.1.2 Random error

164 The errors in \mathbf{r}_j capture local variation that is not trend, such as measurement error and intrinsic variability
 165 within the plots (Besag, 1977; Wilkinson et al., 1983). FieldSimR simulates the vector of random errors as:

$$\mathbf{r}_j \sim \mathbf{N}(\mathbf{0}, \sigma_{r_j}^2 \mathbf{I}_{n_j}), \quad (4)$$

166 where $\sigma_{r_j}^2$ is the random error variance and \mathbf{I}_{n_j} is an identity matrix of order n_j .

167 2.1.3 Extraneous error

168 The errors in \mathbf{e}_j capture extraneous variation predominately induced during the conduct of the trial, such
 169 as serpentine harvesting or spraying and unequal plot dimensions (Gilmour et al., 1997; Stefanova et al.,
 170 2009). This type of variation is assumed to be aligned exclusively with the columns and rows of the trial.
 171 FieldSimR constructs the vector of extraneous errors as the sum of two terms:

$$\mathbf{e}_j = \mathbf{Z}_{c_j} \mathbf{e}_{c_j} + \mathbf{Z}_{r_j} \mathbf{e}_{r_j} \quad (5)$$

172 where \mathbf{e}_{c_j} is the vector of column errors with $n_j \times c_j$ design matrix \mathbf{Z}_{c_j} and \mathbf{e}_{r_j} is the vector of row errors
 173 with $n_j \times r_j$ design matrix \mathbf{Z}_{r_j} . The design matrices are given by $\mathbf{Z}_{c_j} = \mathbf{I}_{c_j} \otimes \mathbf{1}_{r_j}$ and $\mathbf{Z}_{r_j} = \mathbf{1}_{c_j} \otimes \mathbf{I}_{r_j}$.
 174 The column and row errors are simulated as:

$$\mathbf{e}_{c_j} \sim \mathbf{N}(\mathbf{0}, \sigma_{e_{c_j}}^2 \mathbf{I}_{c_j}) \quad \text{and} \quad \mathbf{e}_{r_j} \sim \mathbf{N}(\mathbf{0}, \sigma_{e_{r_j}}^2 \mathbf{I}_{r_j}), \quad (6)$$

175 where $\sigma_{e_{c_j}}^2$ is the column error variance with identity matrix \mathbf{I}_{c_j} and $\sigma_{e_{r_j}}^2$ is the row error variance with
176 identity matrix \mathbf{I}_{r_j} . The column and row error variances are set based on whether column and/or row errors
177 are simulated, such that $\sigma_{e_j}^2 = \sigma_{e_{c_j}}^2 + \sigma_{e_{r_j}}^2$.

178 FieldSimR has the capacity to generate extraneous errors based on zig-zag or random ordering across
179 neighbouring columns and rows. The zig-zag ordering is achieved by alternating positive and negative
180 values between neighbouring columns and rows. The two examples in Figure 3 demonstrate the two types
181 of extraneous variation. The first example demonstrates a zig-zag pattern, with the extraneous errors in
182 odd row numbers being consistently higher than those in even row numbers (mean of +0.37 compared
183 to -0.37). This type of non-stationarity is a classical sign of extraneous variation attributed to systematic
184 management practices, such as serpentine harvesting and spraying. The second example demonstrates a
185 more stochastic pattern in which the errors may be attributed to random processes, such as inaccurate plot
186 trimming resulting in unequal plot dimensions. Interested users may also manipulate the above functionality
187 to simulate intraplot competition, typically observed as a negative correlation between neighbouring rows
188 (Durban et al., 2001; Stringer et al., 2011).

189 2.1.4 Total error

190 FieldSimR constructs the total plot errors in Equation 1 by combining the spatial errors with the random
191 and extraneous errors according to a user-defined ratio. The desired ratio is applied by setting the proportions
192 of spatial error and extraneous error, with the remaining proportion assigned to random error. By default,
193 FieldSimR sets the proportion of spatial error to 0.5 and extraneous error to 0, resulting in a random error
194 proportion of 0.5.

195 2.2 Extension to multiple traits

196 FieldSimR has the capacity to simulate correlated plot errors across multiple traits. The correlation matrix
197 between traits can be set for the spatial, random and extraneous errors, respectively. By default, FieldSimR
198 fits a separable correlation structure between traits and environments (Bančič et al., 2023), but note that
199 different error variances can be set for different environment-within-trait combinations. It is also important
200 to note that when bivariate interpolation is used, the correlation matrix for the spatial error is applied to the
201 z -values at the knot points, not the spatial errors themselves. This is because the spatial errors generated by
202 bivariate interpolation do not have an assumed covariance structure.

3 RESULTS AND DISCUSSION

203 FieldSimR is an R package for simulating plot errors that comprise global and local trend, random error, and
204 extraneous variation. This functionality makes FieldSimR a powerful tool for a wide range of improvement
205 processes, such as the comparison of different spatial modelling approaches. This section demonstrates
206 the simulation and analysis of a field trial which evaluates 100 maize hybrids for two traits across three
207 environments. In the first part, FieldSimR is used to simulate multi-environment plot errors, genetic values
208 and phenotypes for the 100 maize hybrids. In the second part, eight spatial models are compared for their
209 ability to accurately predict the true genetic values of the simulated hybrids and to reliably estimate the
210 true variance parameters of interest.

211 3.1 Simulation example

212 Consider a scenario in which 100 maize hybrids are evaluated for grain yield (t/ha) and plant height (cm)
 213 in a field trial across three environments. The simulation of the maize phenotypes with FieldSimR involves
 214 three steps:

- 215 1. Simulation of plot errors.
- 216 2. Simulation of genetic values.
- 217 3. Simulation of phenotypes by combining the plot errors with the genetic values.

218 3.1.1 Simulation of plot errors

219 Plot errors for grain yield and plant height were simulated assuming independence between traits and
 220 environments. Environments 1 and 2 comprised two blocks each, while environment 3 comprised three
 221 blocks. The blocks were aligned in the column direction (“side-by-side”) and comprised 5 columns and 20
 222 rows for 100 plots in each block. The plots were 8 m long in the column direction by 2 m wide in the row
 223 direction.

224 To obtain target heritabilities of $H^2 = 0.3$ for grain yield and $H^2 = 0.5$ for plant height in all three
 225 environments, the total error variances for the two traits were defined relative to their genetic variances as
 226 described in the Supplementary Script S10. The simulated plot errors comprised spatial error, random error,
 227 and extraneous error terms. The spatial error was simulated using bivariate interpolation with complexity
 228 set to 10 and proportion of spatial error variance set to 0.4 in all three environments. The extraneous
 229 error was simulated using zig-zag ordering across neighbouring rows. The proportion of extraneous error
 230 variance was set to 0.2 in all three environments. This resulted in a proportion of random error variance
 231 given by $1 - (0.4 + 0.2) = 0.4$.

```

error_df <- field_trial_error(n_envs = 3,
                             n_traits = 2,
                             n_blocks = c(2,2,3),
                             n_cols = c(10,10,15),
                             n_rows = 20,
                             block_dir = "col",
                             var_R = c(0.20, 0.28, 0.14, 15.1, 8.5, 11.7),
                             spatial_model = "Bivariate",
                             complexity = 10,
                             plot_length = 8,
                             plot_width = 2,
                             prop_spatial = 0.4,
                             prop_ext = 0.2,
                             ext_dir = "row",
                             ext_ord = "zig-zag",
                             return_effects = TRUE)

```

232
 233 The simulated spatial errors, extraneous errors, random errors, and the total plot errors stored in
 234 `error_df` are presented in Figure 4.

235 3.1.2 Simulation of genetic values

236 Genetic values for grain yield and plant height across three environments were simulated based on
237 an unstructured model for genotype-by-environment (GxE) interaction. The simulation was done in
238 AlphaSimR (Gaynor et al., 2021), using FieldSimR's wrapper functions `unstr_asr_input()` and
239 `unstr_asr_output()`. The R code can be found in Supplementary Script S10. The simulated genetic
240 values can be directly accessed through the package's example data frame `df_gv_unstr`, which was used
241 to simulate phenotypes, as described below. The simulated genetic values for trait 1 in environment 1 are
242 presented in Figure 4.

243 In addition to the unstructured model, FieldSimR provides wrapper functions for simulating genetic
244 values based on a compound symmetry model for GxE interaction. Alternatively, users can provide their
245 own set of genetic values, e.g. through simulation or previously obtained from empirical analyses.

246 3.1.3 Simulation of phenotypes

247 Phenotypes for grain yield and plant height were simulated by combining the simulated plot errors
248 with the genetic values stored in FieldSimR's example data frame `df_gv_unstr`. The genotypes were
249 randomly allocated to plots according to a randomised complete block design (RCBD).

```
pheno_df <- make_phenotypes(gv_df = df_gv_unstr ,  
                             error_df = error_df$plot_df ,  
                             randomise = TRUE)
```

250

251 The phenotypes are presented together with the plot errors and genetic values in Figure 4. Note that
252 FieldSimR does not provide functionality to generate experimental designs other than an RCBD. Users are
253 encouraged to generate alternative experimental designs externally, e.g. with R packages such as `agricolae`
254 (de Mendiburu, 2023), `odw` (Butler, 2021), and `DiGGER` (Coombes, 2020).

255 3.2 Comparison of spatial models

256 The comparison of spatial models is demonstrated using the simulated grain yield data in environment 1.
257 A sequential approach was adopted for model fitting following Gilmour et al. (1997), with global trend
258 and extraneous variation diagnosed using the sample variogram and accounted for using fixed and random
259 model terms. This resulted in eight different spatial models, including a baseline model, three models with
260 a separable first order autoregressive (AR1) process, two models with a tensor product penalized spline
261 (TPS), and two models implementing nearest neighbour (NN) adjustments (Table 1). All models were fitted
262 using `ASReml-R` (Butler et al., 2018) or `SpATS` (Rodríguez-Álvarez et al., 2018), and are summarised in
263 Table 1.

264 The spatial models were evaluated in three ways (Table 2):

- 265 1. The prediction accuracy was calculated using Pearson's correlation coefficient (r) between the
266 simulated true genetic values and the predicted values.
- 267 2. The model fit was assessed using the residual maximum likelihood ratio test (REMLRT) and the
268 Akaike information criterion (AIC).
- 269 3. The reliability was calculated as the bias between the simulated true genetic variance parameter and
270 the estimated parameter.

271 Note that the expected prediction accuracy for the data set is 0.68, based on the simulation parameters.
272 Also note that the REMLRT is based on the positive variance parameter approach of Stram and Lee (1994)
273 and the AIC is based on the full log-likelihood approach of Verbyla (2019), which can compare models
274 with different fixed effects. Typical experimental design and data checks were performed prior to model
275 fitting (Supplementary Figure S5).

276 3.2.1 Baseline model

277 The analyses commenced by fitting a baseline linear mixed model, which included random genotype and
278 block effects and an independent (ID) error model (Table 1). This model reflects a classical complete block
279 analysis that assumes independent genotypes, blocks and residuals. The estimated genetic variance was
280 $\hat{\sigma}_g^2 = 0.02$, which was substantially lower than the true value of 0.09 (bias = 0.07; Tables 2 and 3). The
281 accuracy of the baseline model was also lower than the expected accuracy ($r = 0.65$ compared to 0.68;
282 Table 2).

283 3.2.2 Separable first order autoregressive processes

284 The sequence of models 1-3 comprises three variants of a model that implemented a random genotype
285 effect, block effects and a separable first order autoregressive (AR1) process (Table 1). The separable AR1
286 process represents a random process which assumes correlated residuals in two dimensions, i.e., in column
287 and row direction (Martin, 1990; Cullis and Gleeson, 1991).

288 Model 1 did not include the ID error model. The estimated genetic variance was 0.07, which provided
289 a much better estimate of the true value than the baseline model (bias = 0.02; Tables 2 and 3). Model 1
290 also provided a significantly better fit than the baseline model in terms of LRT ($p < 0.0001$) and AIC
291 (-94.4 compared to -66.7), and a substantially higher prediction accuracy (0.72), as shown in Table 2. The
292 estimated column and row autocorrelations were $\hat{\rho}_c = 0.51$ and $\hat{\rho}_r = 0.23$ (Table 3).

293 Model 2 reintroduced the ID term, which acted as an uncorrelated random error component (Besag,
294 1977). It provided a significantly better fit than Model 1, and was also more accurate (Table 2). The
295 estimated column and row autocorrelations were $\hat{\rho}_c = 0.95$ and $\hat{\rho}_r = 0.87$, which were substantially
296 higher than in Model 1 (Table 3). This indicates that the AR1 process captured (highly correlated) spatial
297 trend, while the ID term captured the remaining random error. The sample variogram in Figure 5a shows a
298 zig-zag pattern between neighbouring rows, with consistently higher semivariances for odd displacements
299 compared to even displacements (also see Supplementary Figure S6). The sill of the variogram shows that
300 the semivariances do not fall within the sample quantiles (Figure 5c). This is a classical sign of extraneous
301 variation attributed to systematic practices, which matches the extraneous error simulated in this dataset.

302 Model 3 fitted a fixed and random row term to model this extraneous variation, following Gilmour et al.
303 (1997). The fixed term was coded as 1 for odd row numbers and 2 for even row numbers (Stefanova et al.,
304 2009). The significance of the fixed term was assessed using a Wald F-test with denominator degrees of
305 freedom ($p < 0.001$; Kenward and Rogers, 1997). The estimated variances in Model 3 were $\hat{\sigma}_s^2 = 0.09$,
306 $\hat{\sigma}_r^2 = 0.08$, and $\hat{\sigma}_{e_r}^2 = 0.05$, which closely matched the true values (Table 3). The estimated column
307 autocorrelation decreased to $\hat{\rho}_c = 0.68$ compared to Model 2. Model 3 provided a significantly better fit
308 than Model 2, and was also more accurate (Table 2). The sample variogram in Figure 5b no longer shows a
309 zig-zag pattern. Instead, a discontinuity is shown at 0 displacement, reflecting the random error variance,
310 followed by a gradual incline in the column direction. This type of non-stationarity is a sign of global
311 trend in the column direction, which matches the spatial error simulated in this dataset. However, the sill
312 of the variogram shows that the semivariances fall within the sample quantiles (Figure 5d). The observed

313 non-stationarity is, therefore, an artefact of the correlated AR1 process, rather than global trend requiring
314 further remediation.

315 3.2.3 Tensor product penalised splines

316 The sequence of models 4-5 used a tensor product penalised spline (TPS), fitted using the SpATS package
317 in R (Rodríguez-Álvarez et al., 2018). A cubic B-spline basis was used with 6 knots in the column direction
318 and 12 knots in the row direction, following Velazco et al. (2017). The TPS included fixed column, row,
319 and interaction terms as well as five random spline components.

320 Model 4 was more accurate and showed a better fit than the baseline model (Table 2), but was less
321 accurate than any of three models implementing the separable AR1 process. Like for Model 2, the sample
322 variogram shows a zig-zag patterns (Supplementary Figure S7), indicating that a better model fit could be
323 obtained by including random row terms.

324 Model 5 is an extension of Model 4 to include random column and row terms. This model is equivalent
325 to the SpATS approach of Rodríguez-Álvarez et al. (2018). Model 5 was more accurate and provided a
326 significantly better fit than Model 4 (Table 2). It was, however, less accurate than the best model using
327 the separable AR1 process (Model 3), despite having five more model parameters (Table 1). The sample
328 variogram of Model 5 no longer shows a zig-zag pattern (Supplementary Figure S8).

329 3.2.4 Nearest neighbour adjustments

330 The sequence of models 6-7 implemented nearest neighbour (NN) adjustments to the phenotypes
331 (Papadakis, 1937; Bartlett, 1978). The adjustments were obtained by averaging over neighbouring plots
332 using the mvngGrAd package in R (Technow, 2015). The grids used for Models 6 and 7 are shown in
333 Supplementary Figure S9. Both models were fitted in ASReml-R, with model terms equivalent to the
334 baseline model (Table 1). Model 6 was more accurate than Model 7, but both models were less accurate
335 than Model 3 (Table 2) and proved insufficient to effectively capture local trend. The estimated variances
336 ranged from $\sigma_g^2 = 0.06$ to 0.08 and $\sigma_r^2 = 0.14$ to 0.17 (Table 3). Note that the model fit criteria in Table 2
337 cannot compare models with different (adjusted) phenotypes, so that the final model was selected based on
338 the ratio of genetic to total phenotypic variance.

4 CONCLUDING REMARKS

339 FieldSimR's capacity to simulate realistic plot errors that capture global field trend, local plot variation,
340 and extraneous variation makes it a flexible and powerful tool for various improvement processes in plant
341 breeding. In contrast to real-world experimental data, FieldSimR enables the efficient and comprehensive
342 assessment of trial designs and analysis models on a large scale, across an extensive array of scenarios.
343 Furthermore, it allows for an unbiased comparison of designs and models for their capacity to generate
344 accurate predictions of genetic values and to reliably estimate variance parameters of interest, as the true
345 values are defined by the user and, therefore, are known.

346 FieldSimR has been extensively deployed as part of the Excellence in Breeding (EiB) initiative to provide
347 guidance on the improvement of field trial design and analysis strategies across numerous CGIAR breeding
348 programmes.

Table 1. Linear mixed models fitted to the simulated maize breeding dataset, Part 1: Summary of model terms.

Model	Terms	Fixed			Random			Residual			
		Col	Row	Col:Row	Hybrid	Block	Col	Row	Spline	AR1	ID
baseline	ID				✓	✓					✓
1	AR1				✓	✓					✓
2	AR1 + ID				✓	✓					✓
3	AR1 + ID + Frow + Rrow		✓		✓	✓		✓			✓
4	TPS + ID	✓	✓	✓	✓	✓			✓		✓
5	TPS + ID + Rcol + Rrow	✓	✓	✓	✓	✓	✓	✓	✓		✓
6	NN ₀ + ID				✓	✓					✓
7	NN ₁ + ID				✓	✓					✓

Presented for each model are the fixed, random, and residual terms. All models also include an overall mean. Model 5 is equivalent to the SpATS approach of Rodriguez-Alvarez et al. (2018). The grids used in the NN adjustments are presented in Supplementary Figure 8. Note: AR1 - separable first order autoregressive process; ID - independent error term; TPS - tensor product penalised spline; NN - nearest neighbour adjustment.

Table 2. Linear mixed models fitted to the simulated maize breeding dataset, Part 2: Model selection criteria.

Model	Fixed	Vars	-2 loglik	REMLRT	AIC	avsed	Accuracy	Bias
baseline	1	3	-70.4		-66.7	0.274	0.65	0.07
1	1	5	-99.1	< 0.0001	-94.4	0.260	0.72	0.02
2	1	6	-113.7	< 0.0001	-103.7	0.249	0.74	0.02
3	2	7	-133.4		-126.6	0.247	0.76	0.02
4	4	8	-110.8		-93.8	0.226	0.69	0.05
5	4	10	-135.7	<0.0001	-116.7	0.245	0.72	0.02
6	1	3	-103.8		-102.0	0.279	0.71	0.01
7	1	3	-94.2		-94.7	0.270	0.70	0.03

Presented for each model are the number of fixed effects and variance parameters, residual deviance, REMLRT, AIC, average standard error of difference (avsed), accuracy and the bias. The selected models are distinguished with *bold font*. Note: The REMLRT is applied sequentially and cannot compare models with different fixed effects. Models 6 and 7 are not comparable because the phenotypes have been adjusted.

REFERENCES

- 349 Akima H (1978) A Method of Bivariate Interpolation and Smooth Surface Fitting for Irregularly Distributed
 350 Data Points. *ACM Transactions on Mathematical Software* 4:148–159, URL [https://doi.org/](https://doi.org/10.1145/355780.355786)
 351 10.1145/355780.355786
- 352 Bančič J, Ovenden B, Gorjanc G, Tolhurst DJ (2023) Genomic selection for genotype performance and
 353 stability using information on multiple traits and multiple environments. *Theoretical and Applied*
 354 *Genetics* 136:104, URL <https://doi.org/10.1007/s00122-023-04305-1>
- 355 Bartlett BM (1978) Nearest neighbour models in the analysis of field experiments. *Journal of the Royal*
 356 *Statistical Society Series B (Methodological)*, 40:147–158, URL [https://doi.org/10.1111/j.](https://doi.org/10.1111/j.2517-6161.1978.tb01657.x)
 357 2517-6161.1978.tb01657.x
- 358 Besag J (1977) Errors-In-Variables Estimation for Gaussian Lattice Schemes. *Journal of the Royal*
 359 *Statistical Society Series B (Methodological)* 39:73–78, URL [https://doi.org/10.1111/j.](https://doi.org/10.1111/j.2517-6161.1977.tb01607.x)
 360 2517-6161.1977.tb01607.x

Table 3. Linear mixed models fitted to the simulated maize breeding dataset, Part 3: REML estimates of variance parameters.

Model	Hybrid	Block	Col	Row	Spline					AR1		ID	
	$\hat{\sigma}_g^2$	$\hat{\sigma}_b^2$	$\hat{\sigma}_{ec}^2$	$\hat{\sigma}_{er}^2$	$\hat{\sigma}_{c_1}^2$	$\hat{\sigma}_{r_1}^2$	$\hat{\sigma}_{c_2}^2$	$\hat{\sigma}_{r_2}^2$	$\hat{\sigma}_{cr}^2$	$\hat{\sigma}_s^2$	$\hat{\rho}_c$	$\hat{\rho}_r$	$\hat{\sigma}_r^2$
baseline	0.02	0.06											0.19
1	0.07	0.00								0.20	0.51	0.23	
2	0.07	0.00								0.40	0.95	0.87	0.09
3	0.07	0.00		0.01						0.10	0.75	0.89	0.08
4	0.04	0.05			0.03	0.03	0.69	0.00	0.07				0.16
5	0.07	0.06	0.00	0.05	0.04	0.02	0.70	0.00	0.08				0.09
6	0.08	0.00											0.14
7	0.06	0.00											0.17
True	0.09			0.04						0.08			0.08

The selected models are distinguished with *bold font*. The true values are given in the final row, with bias given in parentheses. Note: The j indices on the variance parameters have been removed for brevity.

- 361 Besag J, Kempton RA (1986) Statistical Analysis of Field Experiments Using Neighbouring Plots.
362 Biometrics 42:231–251, URL <https://doi.org/10.2307/2531047>
- 363 Box G, Jenkins G (1970) Time Series Analysis: Forecasting and Control. Holden-Day, San Francisco, URL
364 https://doi.org/10.1057/9781137291264_6
- 365 Butler D (2021) odw: Generate optimal experimental designs. URL <https://mmade.org/optimaldesign/>, r package version 2.1.2
- 367 Butler DG, Cullis BR, Gilmour AR, Gogel BJ, Thompson R (2018) ASReml-r reference manual version 4.
368 VSN international URL <https://vsni.co.uk/software/asreml-r>
- 369 Coombes N (2020) DiGGER: DiGGER design generator under correlation and blocking. URL <http://nswdpi.biom.org/austatgen/software>, r package version 1.0.5
- 371 Covarrubias-Pazarán G, Gebeyehu Z, Gemenet D, Werner C, Labroo M, Sirak S, Coaldrake P, Rabbi I,
372 Kayondo SI, Parkes E, Kanju E, Mbanjo EGN, Agbona A, Kulakow P, Quinn M, Debaene J (2022)
373 Breeding Schemes: What Are They, How to Formalize Them, and How to Improve Them? Frontiers in
374 Plant Science 12, URL <https://doi.org/10.3389/fpls.2021.791859>
- 375 Cullis BR, Gleeson GN (1991) Spatial Analysis of Field Experiments - An Extension to Two Dimensions.
376 Biometrics 47:1449–1460, URL <https://doi.org/10.2307/2532398>
- 377 Durban M, Currie ID, Kempton RA (2001) Adjusting for Fertility and Competition in Variety
378 Trials. Journal of Agricultural Science 136:129–140, URL <https://doi.org/10.1017/S0021859601008541>
- 380 Frisch M (2023) Selection tools. URL <http://populati on-geneti cs. uni -gi essen. de/~software/>
- 382 Gaynor RC, Gorjanc G, Hickey JM (2021) AlphaSimR: an R package for breeding program simulations.
383 G3 11, URL <https://doi.org/10.1093/g3journal/jkaa017>
- 384 Gebhardt A, Bivand R, Sinclair D (2023) interp: Interpolation Methods. URL <https://CRAN.R-project.org/package=interp>, r package version 1.1-4
- 386 Gilmour AR, Cullis BR, Verbyla AP (1997) Accounting for Natural and Extraneous Variation in the
387 Analysis of Field Experiments. Journal of Agricultural, Biological, and Environmental Statistics 2:269–
388 293, URL <https://doi.org/10.2307/1400446>

- 389 Gogel B, Welham S, Cullis BR (2023) Empirical comparison of time series models and tensor product
390 penalised splines for modelling spatial dependence in plant breeding field trials. *Frontiers in Plant*
391 *Science* 13, URL <https://doi.org/10.3389/fpls.2022.1021143>
- 392 Green P, Jennison C, Scheult A (1985) Analysis of Field Experiments by Least Squares Smoothing. *Journal*
393 *of the Royal Statistical Society Series B (Methodological)* 47:299–315, URL <https://doi.org/10.1111/j.2517-6161.1985.tb01358.x>
- 395 Kenward MG, Rogers JH (1997) Small Sample Inference for Fixed Effects from Restricted Maximum
396 Likelihood. *Biometrics* 53:983–997, URL <https://doi.org/10.2307/2533558>
- 397 Liu H, Tessema BB, Jensen J, Cericola F, Andersen JR, Sørensen AC (2019) ADAM-Plant: A Software
398 for Stochastic Simulations of Plant Breeding From Molecular to Phenotypic Level and From Simple
399 Selection to Complex Speed Breeding Programs. *Frontiers in Plant Science* 9, URL <https://doi.org/10.3389/fpls.2018.01926>
- 401 Lush JL (1937) *Animal Breeding Plans*. Ames: Iowa State University Press
- 402 Martin RJ (1990) The use of time-series models and methods in the analysis of agricultural field trials.
403 *Communications in Statistics - Theory and Methods* 19:55–81, URL <https://doi.org/10.1080/03610929008830187>
- 405 de Mendiburu F (2023) *agricolae: Statistical Procedures for Agricultural Research*. URL [https://](https://CRAN.R-project.org/package=agricolae,r%20package%20version%201.3-6)
406 [CRAN.R-project.org/package=agricolae,r package version 1.3-6](https://CRAN.R-project.org/package=agricolae,r%20package%20version%201.3-6)
- 407 Papadakis JS (1937) Methode statistique pour des experiences sur champ. *bulletin scientifique Institut*
408 *d'Amelioration des Plantes a Thessaloniki* 23:13–29
- 409 Piepho HP, Boer MP, Williams ER (2022) Two-dimensional P-spline smoothing for spatial analysis of
410 plant breeding trials. *Biometrical Journal* 64:835–857, URL [https://doi.org/10.1002/bimj.](https://doi.org/10.1002/bimj.202100212)
411 [202100212](https://doi.org/10.1002/bimj.202100212)
- 412 Podlich DW, Cooper M (1998) QU-GENE: a simulation platform for quantitative analysis of genetic models.
413 *Bioinformatics* 14(7):632–653, URL [https://doi.org/10.1093/bioinformatics/14.7.](https://doi.org/10.1093/bioinformatics/14.7.632)
414 [632](https://doi.org/10.1093/bioinformatics/14.7.632)
- 415 Rodríguez-Álvarez MX, Boer MP, van Eeuwijk FA, Eilers PHC (2018) Correcting for spatial heterogeneity
416 in plant breeding experiments with P-splines. *Spatial Statistics* 23:52–71, URL [https://doi.org/](https://doi.org/10.1016/j.spasta.2017.10.003)
417 [10.1016/j.spasta.2017.10.003](https://doi.org/10.1016/j.spasta.2017.10.003)
- 418 Stefanova KT, Smith AB, Cullis BR (2009) Enhanced Diagnostics for the Spatial Analysis of Field
419 Trials. *Journal of Agricultural, Biological, and Environmental Statistics* 14:392–410, URL [https://doi.org/](https://doi.org/10.1198/jabes.2009.07098)
420 [10.1198/jabes.2009.07098](https://doi.org/10.1198/jabes.2009.07098)
- 421 Stram DO, Lee JW (1994) Variance Components Testing in the Longitudinal Mixed Effects Setting.
422 *Biometrics* 50:1171–1177, URL <https://doi.org/10.2307/2533455>
- 423 Stringer JK, Cullis BR, Thompson R (2011) Joint Modeling of Spatial Variability and Within-Row
424 Interplot Competition to Increase the Efficiency of Plant Improvement. *Journal of Agricultural,*
425 *Biological, and Environmental Statistics* 16:269–281, URL [https://doi.org/10.1007/](https://doi.org/10.1007/s13253-010-0051-5)
426 [s13253-010-0051-5](https://doi.org/10.1007/s13253-010-0051-5)
- 427 Technow F (2015) R package mvngGrAd: moving grid adjustment in plant breeding field trials
- 428 Velazco JG, Rodríguez-Álvarez MX, Boer MP, Jordan DR, Eilers PHC, Malosetti M, van Eeuwijk FA
429 (2017) Modelling spatial trends in sorghum breeding field trials using a two-dimensional P-spline mixed
430 model. *Theoretical and Applied Genetics* 130:1375–1392, URL [https://doi.org/10.1007/](https://doi.org/10.1007/s00122-017-2894-4)
431 [s00122-017-2894-4](https://doi.org/10.1007/s00122-017-2894-4)

- 432 Verbyla AP (2019) A note on model selection using information criteria for general linear models estimated
433 using REML. *Australian & New Zealand Journal of Statistics* 61:39–50, URL [https://doi.org/](https://doi.org/10.1111/anzs.12254)
434 [10.1111/anzs.12254](https://doi.org/10.1111/anzs.12254)
- 435 Wilkinson GN, Eckert SR, Hancock TW, Mayo O (1983) Nearest Neighbour (NN) Analysis of Field
436 Experiments. *Journal of the Royal Statistical Society Series B (Methodological)* 45:151–211, URL
437 <https://doi.org/10.1111/j.2517-6161.1983.tb01240.x>
- 438 Younis OG, Turchetta M, Ariza Suarez D, Yates S, Studer B, Athanasiadis IN, Krause A, Buhmann
439 JM, Corinzia L (2023) ChromaX: a fast and scalable breeding program simulator. *bioRxiv* URL
440 <https://doi.org/10.1101/2023.05.29.542709>

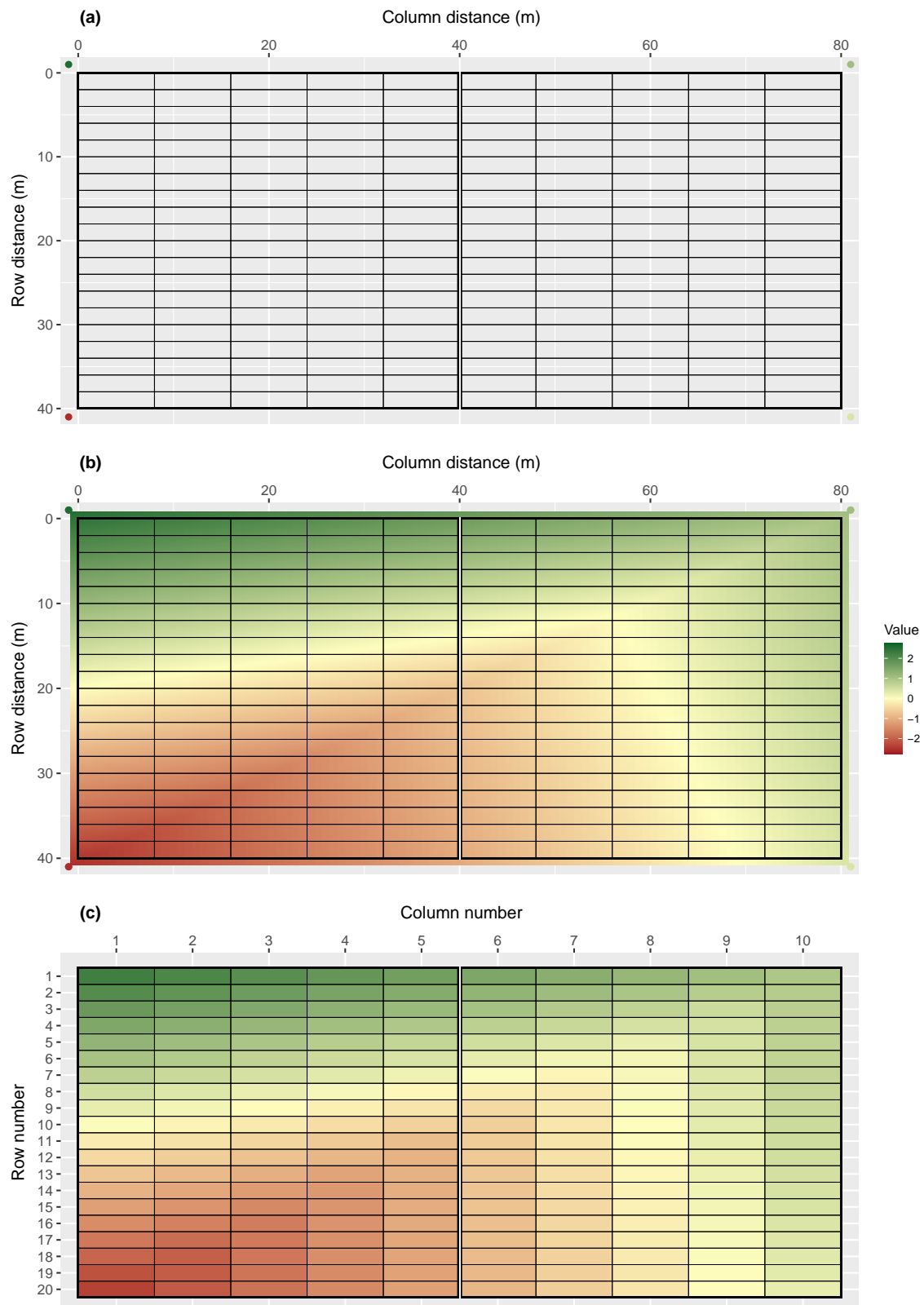


Figure 1. Demonstration of how FieldSimR generates spatial errors using bivariate interpolation: (a) the two-dimensional lattice of plots is constructed with four interpolation (knot) points placed outside the four corners, (b) the continuous array between the knot points is interpolated using bivariate interpolation, which produces a smooth continuous surface, (c) a single error value is assigned to each plot by averaging over the continuous surface within each plot.

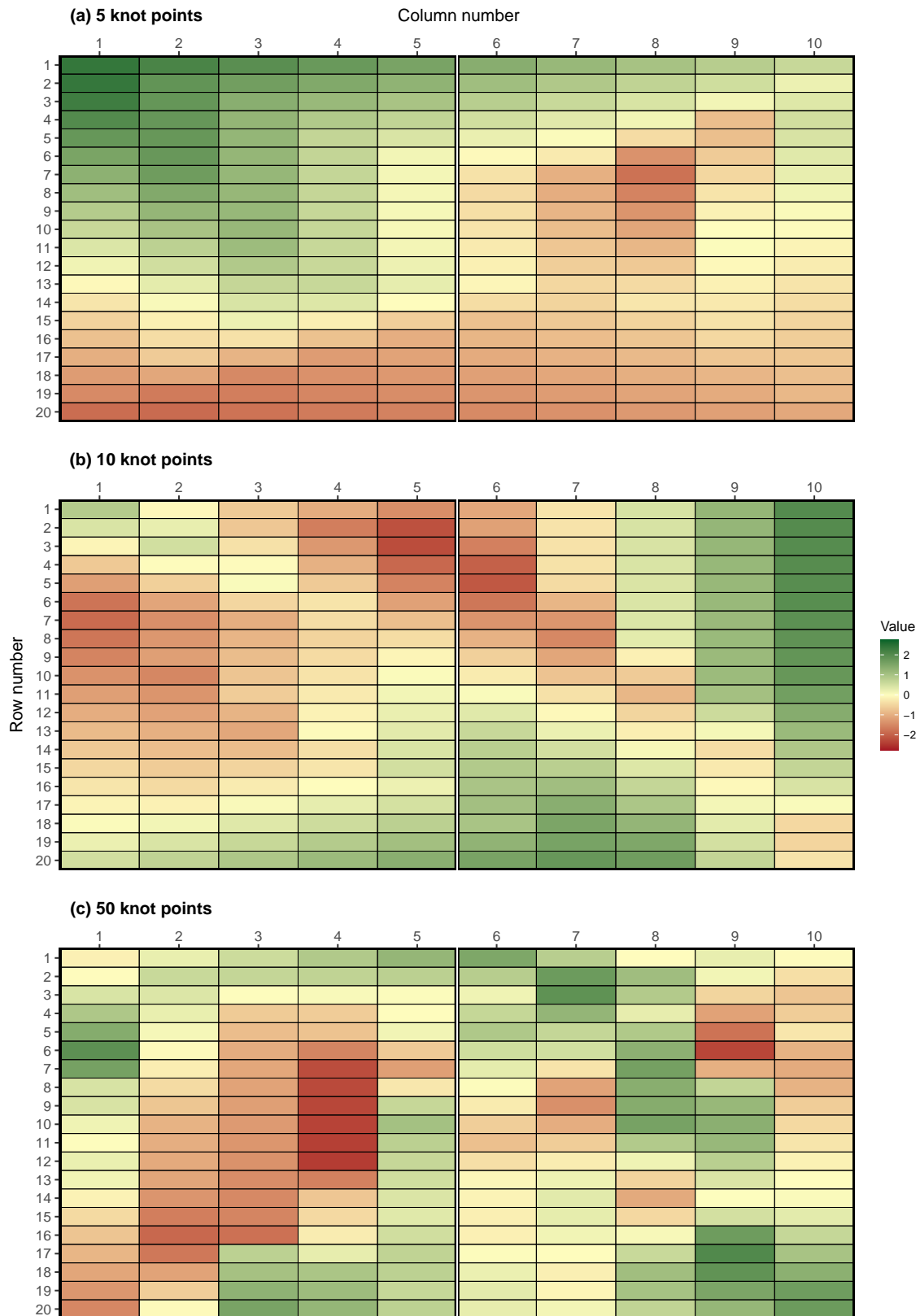


Figure 2. Examples of spatial errors generated using bivariate interpolation with (a) 5, (b) 10, and (c) 50 knot points. These options are set using `complexity = 5, 10, and 50`. The coordinates of the knot points are presented in Supplementary Figure 2.

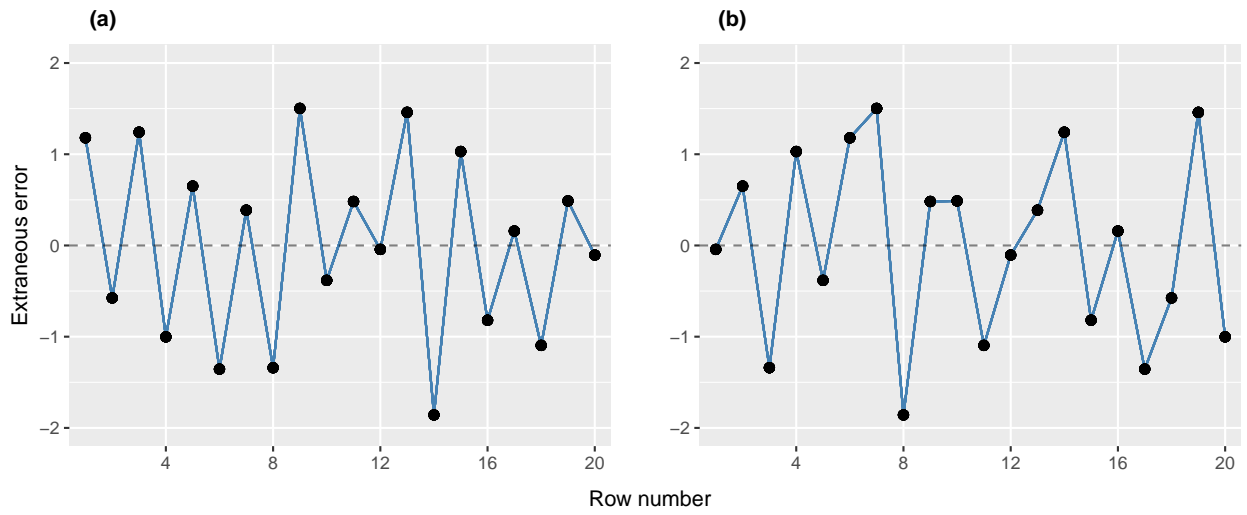


Figure 3. Examples of extraneous errors generated using (a) zig-zag or (b) random ordering.

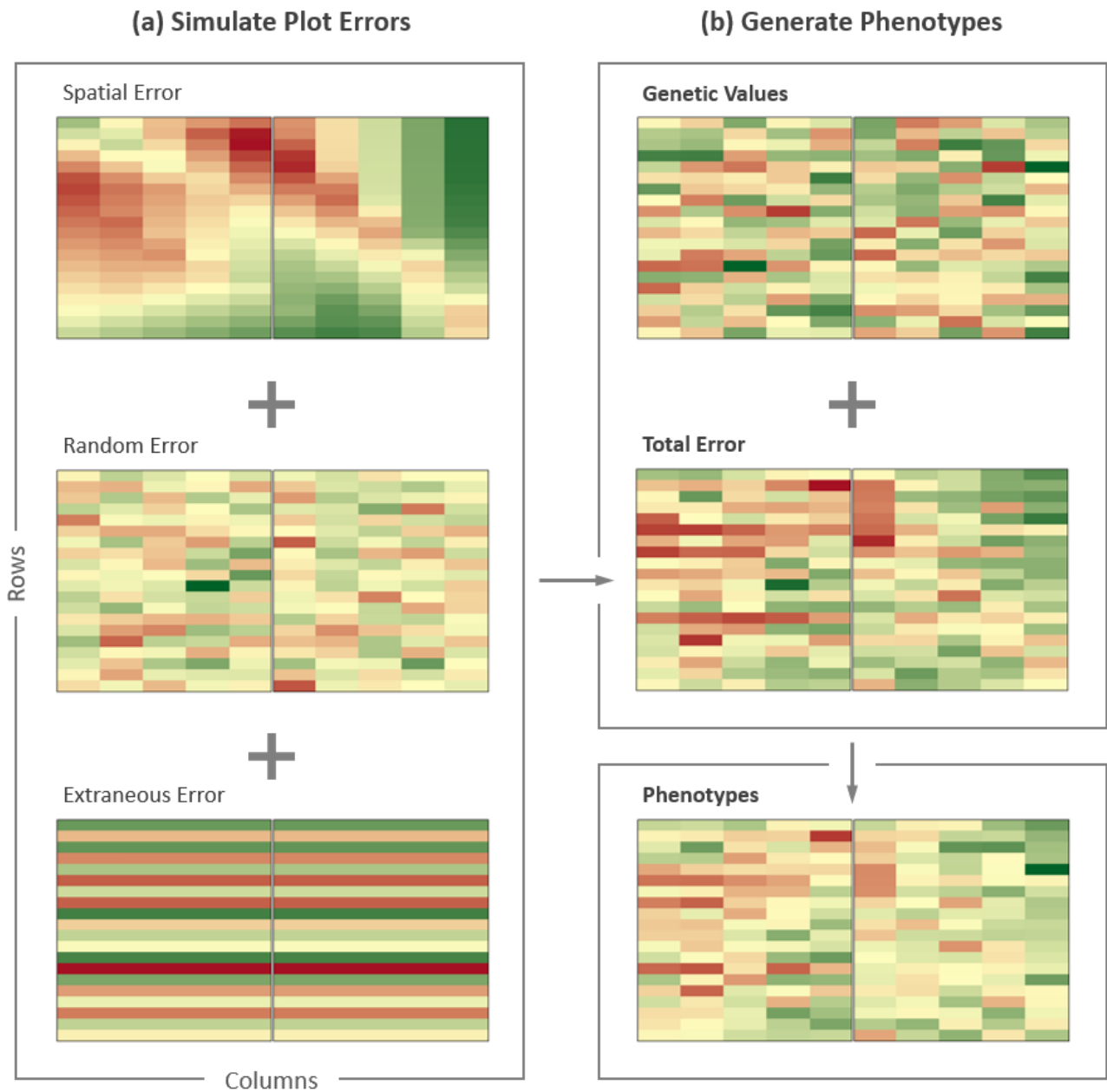


Figure 4. Demonstration of how FieldSimR generates phenotypes: (a) the plot errors are constructed by combining the spatial errors with the random and extraneous errors at a user-defined ratio, (b) the phenotypes are generated by combining the plot errors with the true genetic values obtained from AlphaSimR. A randomised complete block design is used to allocate genotypes to plots.

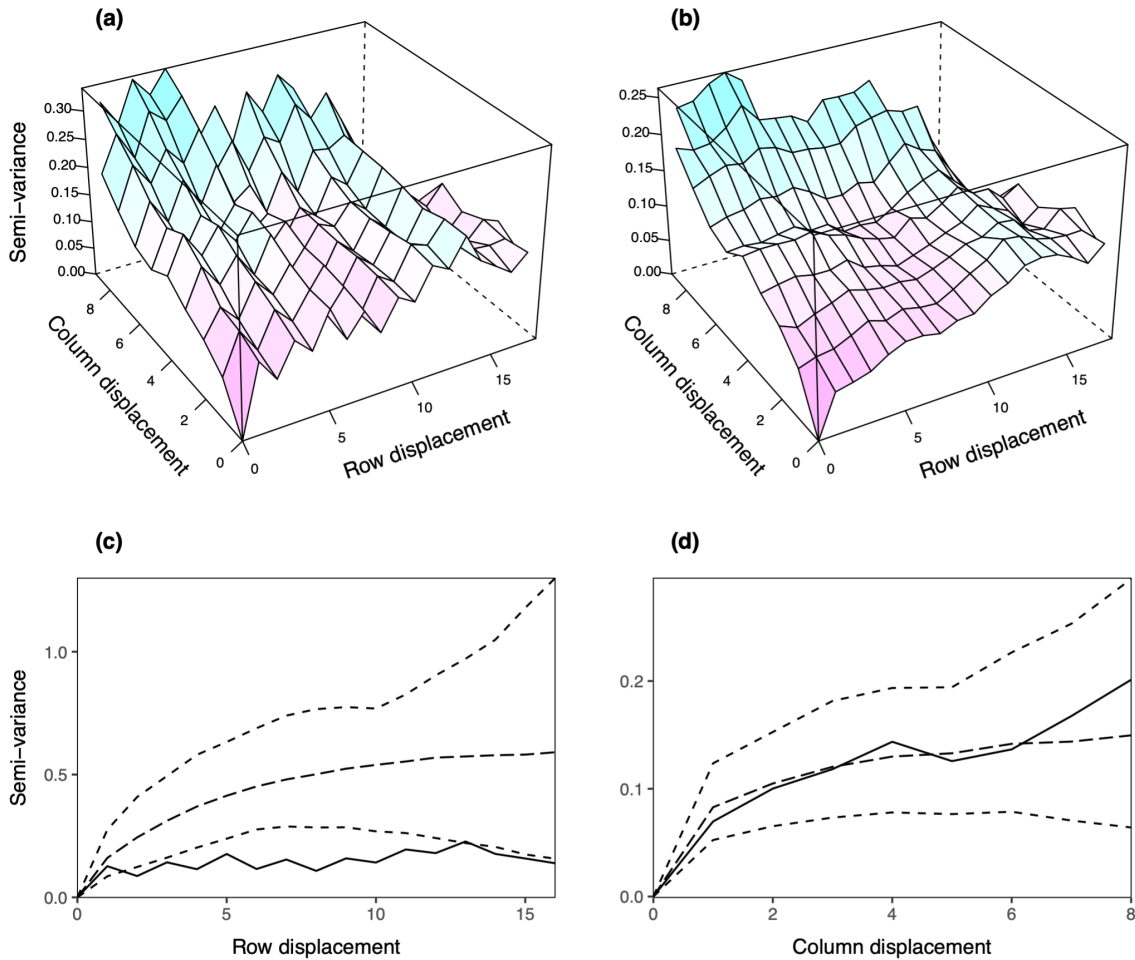


Figure 5. Sample variograms for the AR1 based models fitted to the simulated plot data in Figure 4: (a) Model 2: AR1+ID and (b) Model 3: AR1+ID+Frow+Row. The corresponding variogram sills are presented in (c) for Model 2 and (d) for Model 3. Note: Only semi-variances based on more than 30 pairs are shown. AR1 - separable first order autoregressive process; ID - independent error term, Frow - fixed row term; Row - random row term.